Journal of Non-Crystalline Solids 32 (1979) 405–419

RAMAN SCATTERING IN PURE AND HYDROGENATED AMORPHOUS GERMANIUM AND SILICON

Dionisio BERMEJO * and Manuel CARDONA
Max-Planck-Institut für Festkörperforschung, Stuttgart, FRG

Received 17 August 1978

The Stokes Raman spectra of pure and hydrogenated amorphous germanium and silicon are discussed. First- and second-order structures due to the vibration of Ge–Ge and Si–Si bonds and also first-order structures due to Ge–H and Si–H bonds are observed. The resonance behaviour and the polarization ratio of the observed structures are presented and interpreted in terms of a dielectric constant-bond polarizability model.

1. Introduction

Crystalline germanium and silicon have only one Raman active phonon mode. This mode is three-fold degenerate and has T_{2g} (or $\Gamma_{25'}$) symmetry, Its frequency is, at room temperature, 520 cm^{-1} for Si and 300 cm^{-1} for Ge. The wave vector k of the mode which is excited with conventional lasers is negligible as compared to the size of the Brillouin zone: other phonons with finite k are Raman forbidden as a result of the translational symmetry. These phonons can, however, be observed as two phonon processes in the second-order Raman spectrum. In this case only the *sum* of the k's of the two phonons must be vanishingly small and hence the whole Brillouin zone contributes to the Raman spectrum [1–3]. In amorphous Ge and Si the translational invariance is broken by the lack of long-range order. As a result the k-conservation selection rule breaks down and all phonon modes become first-order Raman allowed [4]. The tetrahedral short-range order is preserved in a-Ge and a-Si: thus the density of vibrational states of these materials is simply a broadened version of that of their amorphous counterparts: the first-order Raman spectra of a-Si and a-Ge reflect that density of states modulated by transition matrix elements and statistical factors [5]. Second-order features due to Raman scattering by two phonons have also been observed recently in a-Si [6].

Beside the kinematical factors just mentioned, the *strength* of the Raman spectra of semiconductors contains information about electron–phonon interaction [7].

* Permanent address: Instituto de Estructura de la Materia, Serrano 119, Madrid, Spain.

For crystalline materials this information is expressed by electron–phonon coupling constants or deformation potentials which are best obtained in resonance Raman experiments (i.e. measurement of scattering cross section versus photon energy near an optical critical point). For amorphous materials a description in terms of critical points is not possible. The theory so far available consists of a description in *real space* in terms of bond polarization models [8]. Resonance experiments recently reported for a-Si [6], help to ascertain whether one or several different electron–phonon coupling mechanisms are involved.

The properties and structure of hydrogen doped a-Si and a-Ge have been of considerable interest ever since the work of Spear and LeComber on the doping of a-Si produced by a glow discharge in SiH_4 containing either PH_3 (n-type) or B_2H_3 (p-type) [9]. Hydrogen atoms saturate broken bonds in the amorphous materials and can be identified by means of their infrared and Raman vibronic spectra [10,11].

In this paper we present the Raman spectra of pure and hydrogenated (deuterated) a-Ge and a-Si produced by sputtering in a H_2–Ar (D_2–Ar) mixture with several partial pressures of $H_2(D_2)$. Results for a glow discharge produced "polysilane" sample [10] are also included. Structures due to scattering by one phonon, two phonons, hydrogen (deuterium) bond stretching and wagging are observed. Especial emphasis is paid to the depolarization ratios of the observed structures, and their strengths as compared with that of the first-order phonon in the corresponding crystalline materials. The resonances of the scattering cross section of the TO one-phonon structure and the hydrogen bond structures in the region between 1.5 and 3.7 eV are also reported and interpreted with a simple polarizability model. The spectral dependence of the real and imaginary parts of the dielectric constant required to evaluate this model are obtained by means of pseudo-brewster angle measurements [12].

2. Experiment

2.1. Sample preparation

Four a-Si samples were used in the experiments discussed here. Sample a-Si (1) was prepared by rf sputtering in pure Ar atmosphere (0.04 Torr) and was equivalent to sample 32 of ref. [10] Samples a-SiH_x(2) and a-SiH_x(3) were prepared by the same procedure in an Ar-H_2 mixture (0.04 Torr) with a partial pressure of H_2 of 1% and 10% respectively. Their thicknesses were 5000 and 11000 Å. The fourth sample, a-SiH_x(3), was equivalent to sample 78 of ref. [10] (polysilane): it was prepared by glow discharge decomposition of silane on a substrate at 25°C as described in ref. [10]. Five a-Ge samples, all prepared by rf sputtering, in Ar–H_2 mixtures (0.02 Torr) with various partial pressures of H_2 on a substrate at room temperature, were measured. Their characteristics are given in table 1. The samples

Table 1
Characteristics of a-GeH_x samples used in the present experiments

Sample number	partial [a] H_2 pressure	N_H [b] (10^{22} cm^{-3})	x [c]	d [d] (microns)	n [e] (1.9 eV)	n [f] (ir)
1	0		0	0.18	4.3	3.8
2	1%		0.02	0.41	3.7	3.5
3	10%	0.9	0.20	0.34	3.0	2.9
4	25%	0.9	0.20	0.30	3.4	3.5
5	70%	1.3	0.30	0.10	4.3	3.0

a) During sputtering.
b) Concentration of hydrogen determined from the ir bond stretching bands (see next paper).
c) Calculated from N_H and the germanium concentration of crystalline germanium (4.5×10^{22} cm^{-3}). The Ge concentration of a-GeH_x should be somewhat lower than 4.5×10^{22} cm^{-3}).
d) Thickness from Tallysurf measurements.
e) From pseudo-brewster measurements.
f) From ir fringes.

were prepared on (111) oriented and polished single crystal silicon substrates slightly wedged (0.3°) so as to avoid interference fringes due to the substrate in ir measurements. Their thicknesses were determined with a Tallysurf [13]. The typical accuracy of the thickness determination was ±200 Å. Some samples for optical absorption measurements in the visible and near ir were prepared on suprasil substrates.

2.2. Raman measurements

The Raman spectra were excited with various lines of Spectra Physics model 164 Argon, and 171 Krypton ion lasers with a power ⩽300 mW focused on the sample with a cylindrical lens so as to avoid heating. For the resonance experiments a Spectra Physics model 185 He–Cd laser (4416 Å, 90 mW) was also utilized.

As a spectrometer we used a Spex provided with holographic gratings. The detector was an RCA C31034 photonmultiplier in the photon counting mode. The counts were stored in a multichannel analyzer. The relative Raman cross sections were determined for each laser line by comparison with the Raman active mode of a CaF_2 crystal (323 cm^{-1}) which is assumed to have a spectral dependence of the cross section like the fourth power of the laser frequency in the region of our measurements as it is transparent up to 10 eV.

2.3. Other measurements

The resonance data (cross section as a function of laser frequency ω_L) must be corrected for the varying absorption coefficient of the sample [14]. The optical

constants of pure a-Si and a-Ge, needed to perform this correction, are available in the literature [15,16]. Those of the hydrogenated samples were determined using the pseudobrewster angle technique [12] which consists in measuring the angle of incidence at which the reflection coefficient for "p"-polarization has a minimum and the reflectivity at that minimum. These measurements were performed in a goniometer with a Xe lamp. A correction for a possible oxide layer, particularly important at long wavelengths [12], was performed by matching the absorption coefficient to that obtained from transmission in the region of relatively low absorption ($\alpha \lesssim 10^5$ cm^{-1}). In this region the absorption coefficient was also determined by measuring the attenuation of the Raman signal of the single crystal Si substrate measured through the amorphous film. Typical oxide layers obtained under the assumption of a non-dispersive refractive index $n_{\text{Si oxide}} = 1.46$, $n_{\text{Ge oxide}} = 2.0$ were 70 Å for a-Si and 40 Å for a-Ge.

Infrared absorption measurements were also performed. The results for $SiH_x(4)$ are discussed in ref. [10] those for $GeH_x(3)$ and $GeH_x(5)$ in the next paper. The strength of the infrared bands enabled us to determine the hydrogen concentrations listed in table 1 (see next paper). A hydrogen concentration of 3×10^{22} cm^{-3} ($x \sim 0.5$) was reported in ref. [10] for $SiH_x(4)$. From the strength of the infrared bands we obtained for $SiH_x(3)$ $x \approx 0.15$. The hydrogen concentration found by this method for the GeH_x samples are listed in table 1.We have also listed in this table the values of the refractive index n found from the interference fringes observed in the infrared ($\omega \leqslant 2000$ cm^{-1}) using the Tallysurf thickness and the values of n measured at $\omega = 1.9$ eV using the pseudo-brewster method.

3. Results

The polarized (||) and depolarized ($\perp$) first and second-order Raman spectra (stokes) of the pure a-Si sample are shown in fig. 1 for $\omega_L = 2.54$ eV. These data are basically the same as those reported in ref. [6]. They yield a depolarization ratio $\rho = 0.53 \pm 0.05$ for all of the observed structures. Differences between || and $\perp$ scattering observed below 450 cm^{-1} are structureless and thus attributed to a background of unknown origin (Rayleigh). The background was substracted for estimating ρ. This value of ρ is considerably less than the complete depolarization reported in ref. [8] (the maximum theoretical value of ρ is $\frac{3}{4}$ and is called *complete* depolarization). It was found that ρ is slightly dependent on ω_L (see fig. 2): it dropts to ≈ 0.42 at the lowest photon energies measured (1.55 eV). We show in fig. 3 the polarized first-order spectra of the two sputtered a-SiH_x samples [sample (2), $x <$ 11%; sample (3), $x \approx 11\%$). These spectra are very similar to those of fig. 1 (the polarized spectrum of fig. 1 is reproduced in fig. 3 for comparison). The main difference between the spectra of the hydrogenated and the non-hydrogenated samples of fig. 3 is the decrease of the TA, LA and LO structures with increasing hydrogen content. Such an effect was also reported in ref. [6] for sample a-Si (4),

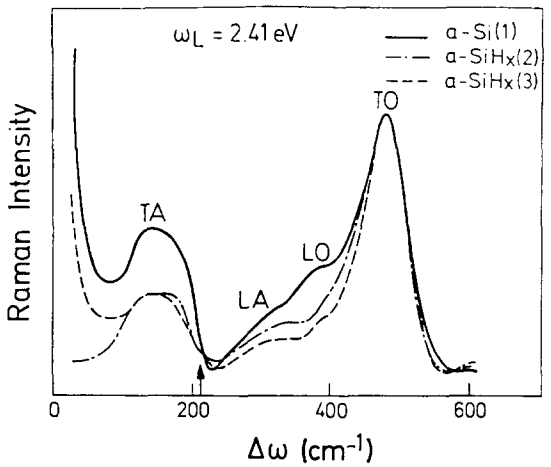

Fig. 1. Stokes Raman spectrum of pure amorphous silicon obtained for parallel (∥) and perpendicular (⊥) scattering configurations. These and all subsequent data were taken at room temperature.

where the weak structure which appears at $\Delta\omega \approx 210\ \mathrm{cm}^{-1}$ can also be observed.

The dependence of the scattering cross section of the spectra of fig. 3 [a-SiH_x(2), a-SiH_x(3)] and that of SiH_x(4) on photon energy ω_L, integrated between 200 and 600 cm^{-1}, and relative to that of CaF_2, is shown in fig. 4 (points). We have also included in this figure the cross section of the bond stretching Raman bands of a-SiH_x(3) and a-SiH_x(4) [10]. With the exception of the stretching band of a-SiH_x(4), the shapes of all resonance curves in fig. 4 are very similar. The Si–H bond-stretching band of the polysilane sample [a-SiH(4)] shows no resonance at all in the region of our measurements.

The polarized spectra of pure a-Ge and two hydrogenated samples are shown in

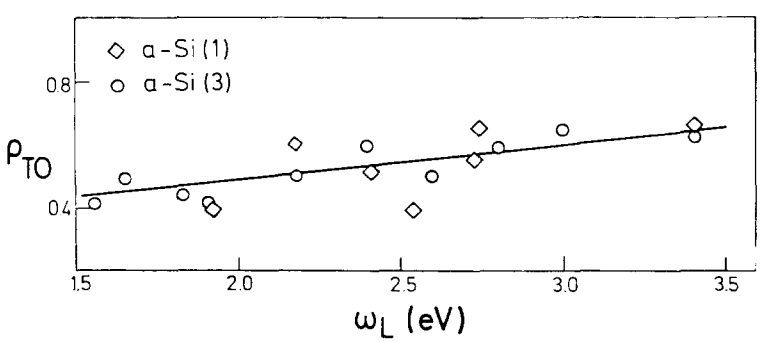

Fig. 2. Depolarization ratios of the TO structure in fig. 1 for several laser frequencies.

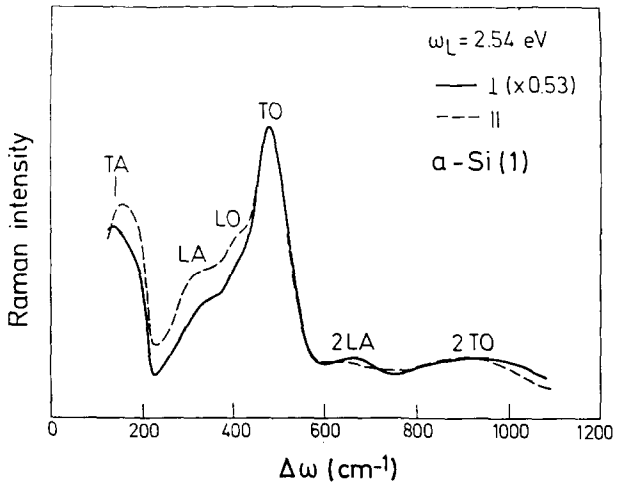

Fig. 3. Stokes Raman spectra (∥-configuration) of pure amorphous silicon [a-Si(1)] and two sputtered hydrogenated samples.

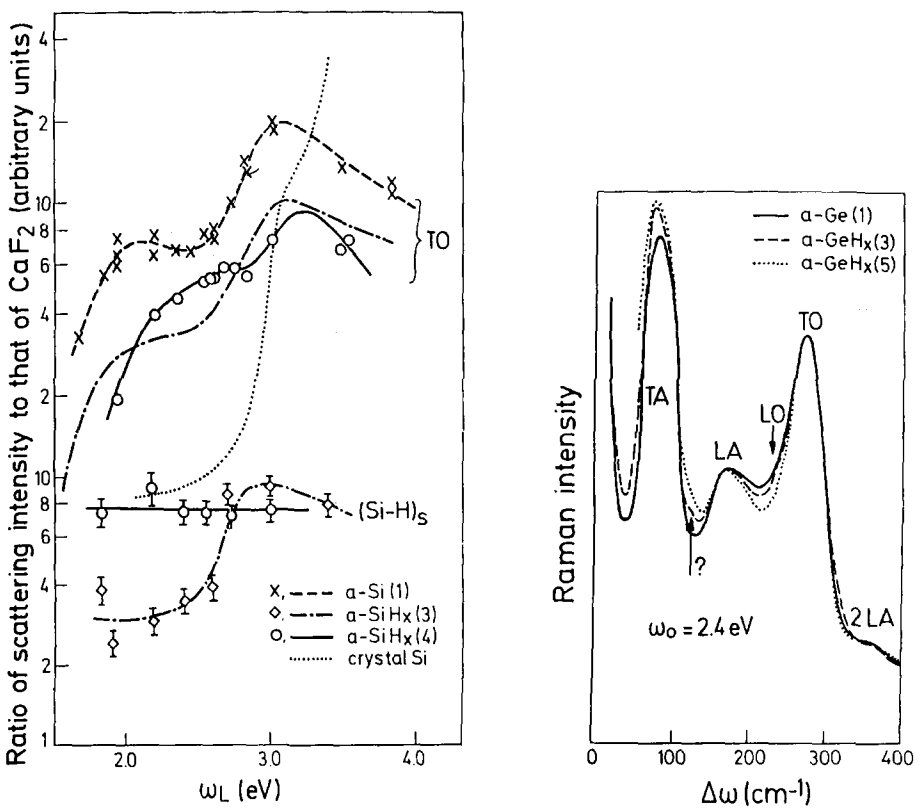

Fig. 4. Stokes scattering cross section (relative to CaF_2) of several structures observed in pure and hydrogenated a-Si as a function of laser frequency. The dotted curve represents the resonant behaviour of single crystal silicon taken from ref. [3].

Fig. 5. Raman spectra of pure a-Ge and two hydrogenated a-Ge samples between 30 and 400 cm^{-1}.

fig. 5 for $30 < \Delta\omega < 400\ \text{cm}^{-1}$. The depolarization ratios were also measured for these samples and found to be $\rho \approx 0.59 \pm 0.05$ at 2.18 eV and $\rho \approx 0.48 \pm 0.05$ at 1.8 eV. We note that some decrease in the scattered intensity of the LO structure with increasing x also seems to occur in this case, although the situation is not as clear as in fig. 3: The LO structure is not as well defined for a-Ge as for a-Si. Fig. 6 shows the polarized spectra for $\Delta\omega > 300\ \text{cm}^{-1}$ of the samples of fig. 5 plus a deuterated one (a-GeD$_x$) prepared under the same conditions as a-GeH$_x$ except for the replacement of H_2 by D_2. Fig. 6 contains 2 LA, 2 LO, and 2 TO second-order structures, analogous to those of fig. 1 but appropriately shifted to lower $\Delta\omega$ as a result of the heavier mass of Ge. It also contains structures which appear upon either hydrogenation or deuteration. On the basis of refs. [10] and [11] and the following paper we attribute these structures to Ge–H bond wagging and bond stretching modes. The bond stretching modes $(\text{Ge–H})_s$ are split into two, a fact already known from the infrared spectra [11] and also observed in the Raman spectrum of a-SiH$_x$ [10]. The polarization ratio of the wagging modes was found to be $\rho_{(\text{Ge–H})_w} = 0.45 \pm 0.1$. The $(\text{Ge–H})_s$ modes were too weak to be seen in $\perp$ configuration. For the corresponding mode of Si $\rho_{(\text{Si–H})_s} = 0.2$ [10].

We show in fig. 7 the dependence on photon energy of the scattering cross section of the first-order scattering between 130 and 330 cm^{-1} (Ge–Ge modes, mainly TO) for samples a-Ge (1), a-GeH$_x$(3), and a-GeH$_x$(5) and that of the

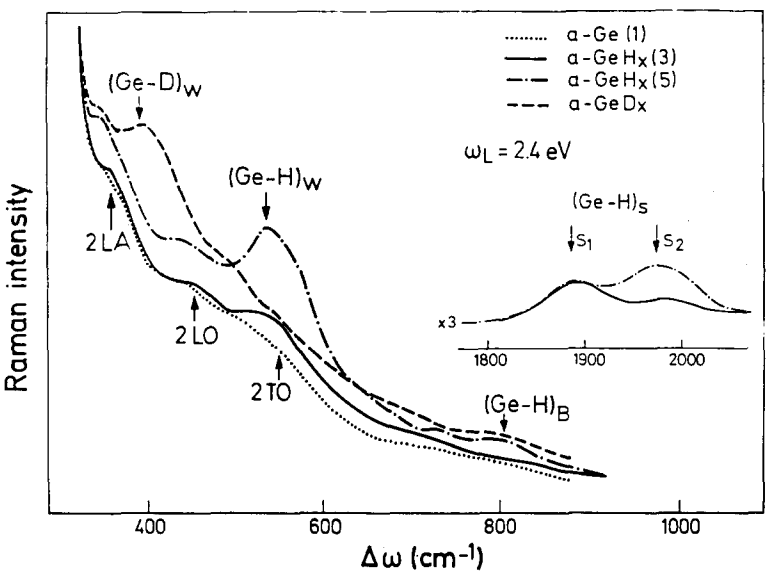

Fig. 6. Raman spectra of pure a-Ge, two a-GeH$_x$ and one a-GeD$_x$ samples above 300 cm^{-1} showing second-order Ge–Ge structures and first-order Ge–H (or Ge–D) bond wagging and stretching modes.

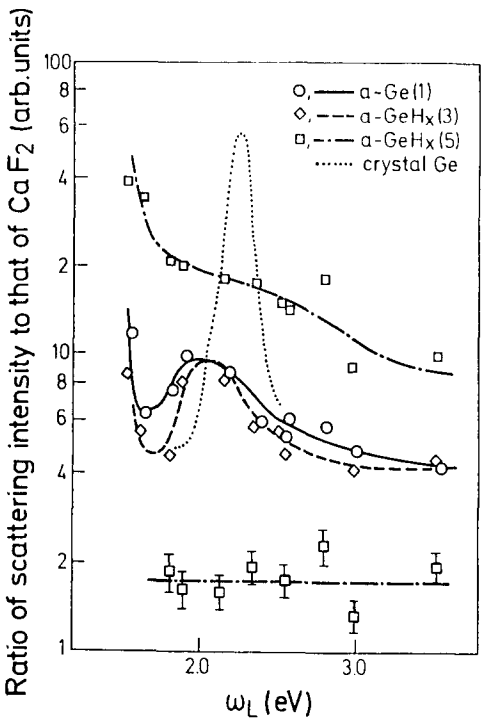

Fig. 7. Stokes scattering cross section (relative to CaF_2) of several structures of figs. 5 and 6 as a function of laser frequency. The lowest curve represents the $(Ge-H)_w$ modes while the remaining curves correspond to the Ge–Ge vibrations.

$(Ge-H)_w$ band for a-GeH_x(5). The behaviour of the Ge–Ge modes is rather similar for the three samples while the wagging mode does not show any frequency dependence for heavily hydrogenated a-GeH_x(5), the only sample for which the wagging band was strong enough to measure its resonance. Unfortunately the stretching band was too weak to measure its resonance even for this sample.

4. Discussion

4.1. Observed modes

The frequency of the peak or center of all bands observed in the Raman spectra of pure and hydrogenated a-Ge and a-Si are listed in table 2 together with the frequencies of the Raman phonons of the corresponding crystalline materials. The second-order features peak to within about 5% at twice the frequencies of the corresponding first-order structures. The hydrogenated samples exhibit Si–H bond

Table 2
Frequencies (in cm^{-1}) of the peak or center of various bands observed in the Stokes Raman spectra of a-Ge, a-Si and their hydrogenated counterparts. w represents hydrogen bond wagging and s-hydrogen bond stretching bands. Also ratio of the equivalent frequencies of Si and Ge and values of this ratio multiplied by the square root of the atomic mass ratio $(m_{Ge}/m_{Si})^{1/2}$

	TA	?	LA	LO	TO	T_{25}' (crystal)	2 LA	2 LO	2 TO	R	W	S_1	S_2
Si	150	215	310	380	480	520	660	–	960	610	660	2030	2100
Ge	80	125	177	230	278	300	360	450	550	540	565	1890	1975
$\frac{\omega_{Si}}{\omega_{Ge}}$	1.88	1.72	1.75	1.65	1.73	1.73	1.83	–	1.74	1.13	1.17	1.08	1.06
$\frac{\omega_{Si}}{\omega_{Ge}} \frac{m_{Ge}}{m_{Si}}$	1.17	1.07	1.09	1.03	1.07	1.07	1.10	–	1.08				

wagging and stretching bands, the stretching bands being a doublet for both Ge and Si. In agreement with ref. [10] we identify the upper of the two stretching bands S_2 with $SiH_2(GeH_2)$ groups (two hydrogens bonded to one Si(Ge) and the lower S_1-band with SiH(GeH) groups. The bending modes, which should be associated with SiH_2 GeH_2 groups, are too weak to be observed. As will be shown in the next paper, sample $GeH_x(3)$ has a fraction $x \approx 0.07$ of hydrogen atoms as GeH_2 and $GeH_x(5)$ $x \approx 0.15$ in this form. A similar estimate of the concentration of GeH_2-bonded hydrogen is obtained from the ratio of the areas under the two components of the $(Ge–H)_s$ peak of fig. 6.

We have also listed in table 2 the ratio of the frequencies of a given mode in a-Si to that of a-Ge $[\omega(Si)/\omega(Ge)]$ and this ratio renormalized by means of the square root of the ratio of the corresponding masses $[(\omega(Si)/\omega(Ge))x(m_{Si}/m_{Ge})$. The latter ratio should be close to one as it represents the ratio of the corresponding mode spring constants. While we see in table 2 that this is indeed the case we find a systematically higher value ($\sim$1.1) for this ratio. This deviation can be easily explained as due to differences in the Si–Si and Ge–Ge bond lengths or, correspondingly, Si–H and Ge–H. The spring constants should vary like the -1.5 power of that bond length [17]. Thus the renormalized frequency ratio of table 2 should equal:

$$\left(\frac{a_0(\mathrm{Ge})}{a_0(\mathrm{Si})}\right)^{1.5} = \left(\frac{5.65}{5.43}\right)^{1.5} = 1.06,$$

in reasonable agreement with the listings of table 2 (the ratio of Ge–H to Si–H bond lengths is practically the same as that of the lattice constants a_0(Ge) to a_0(Si) [18]). We also note that the unidentified structure labelled with a question mark in table 2 must be related to Ge–Ge or Si–Si bonds as it scales like the square root of the mass ratio.

4.2. Resonance Raman scattering

Within the framework of the polarizability theory the stokes scattering cross section is given by:

$$\sigma \propto \omega_L^4 \, |\mathrm{d}\epsilon/\mathrm{d}u|^2 \, |\langle n_B + 1 \, | u \, | n_B \rangle|^2, \tag{1}$$

where ϵ is the complex dielectric constant, u the normal coordinate of the phonon and n_B the Bose–Einstein statistical factor. The plots of figs. 4 and 7 represent actually σ/ω_L^4 as the measurements have been performed relative to CaF_2. If we assume that one single dispersion frequency or gap ω_0 determines ϵ, a reasonable assumption in view of the nearly Lorentzian shape of ϵ [15], we can write eq. (1) in the form:

$$(\sigma/\omega_L^4) \propto |\mathrm{d}\epsilon/\mathrm{d}\omega|^2 \, |\mathrm{d}\omega_0/\mathrm{d}u|^2 (n_B + 1), \tag{2}$$

where we have further assumed that ϵ is modulated by changes in ω_0 and not by

changes in the transition matrix elements. The quantity $d\omega_0/du$ represents an average deformation potential.

We have plotted in fig. 2 of ref. [6] the frequency dependence of the scattering cross section obtained with eq. (2) using for the real (ϵ_1) and imaginary (ϵ_2) parts of ϵ the data of ref. [15]. The calculated curve represents well the experimental data of the pure sample and also of the lightly hydrogenated a-SiH_x(3) sample. The "polysilane" sample exhibits a slightly shifted resonance curve.

We have also evaluated eq. (2) for the a-SiH_x(3) sample from pseudo-brewster angle data for ϵ_1 and ϵ_2 shown in fig. 8. The results are compared with experimental cross sections for polarized scattering in fig. 9.

We note in fig. 4 that the $(Si-H)_s$ modes of the lightly hydrogenated sample show a resonance behaviour similar to the Si–Si vibrations. The a-SiH_x(5) sample (polysilane), however, shows a nearly frequency independent $(Si-H)_s$ vibration. Similar behaviour is observed for the Ge–H wagging mode of a heavily hydrogenated sample in fig. 7. This fact can be interpreted by considering the electronic structure of hydrogen singly and multiply bonded to silicon as calculated by Ho et al. [20]. For singly bonded silicon these authors found rather unlocalized electronic wave functions which extend to Si–Si backbonds. For $-SiH_3$ they found a rather localized behaviour of the wave function within the Si–H bonds. Correspondingly we can interpret our resonance experiments by postulating that the vibration of the Si–H bonds modulates the polarizability of their Si–Si neighbouring bonds if hydrogen is singly bonded but not if it is multiply bonded.

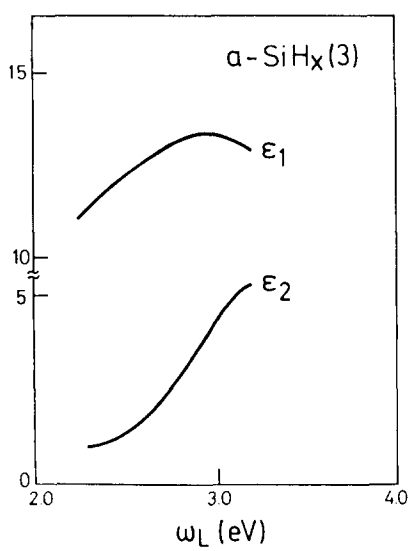

Fig. 8. Real (ϵ_1) and imaginary (ϵ_2) parts of the dielectric constant of a-SiH_x(3) as a function of photon energy as determined with the pseudo-brewster angle method.

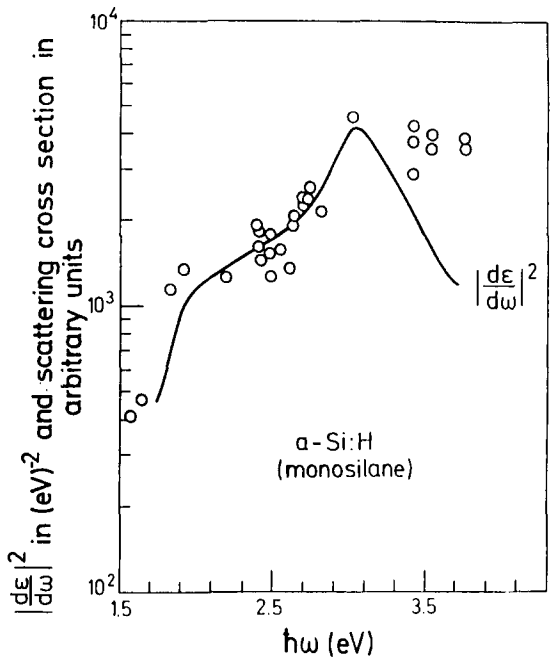

Fig. 9. Comparison of the resonance observed in the TO Raman cross sections of a-SiH_x(3) with the predictions of the dielectric theory $|d\epsilon/d\omega|^2$ based on the ϵ of fig. 7.

We can also interpret the resonance behaviour found for pure a-Ge in fig. 7 with either existing data for ϵ or with our pseudo-brewster angle measurements. We show in fig. 10 a comparison of the experimental data with $|d\epsilon/d\omega|^2$ obtained from ϵ_1 and ϵ_2 of ref. [16]. We compare in fig. 11 the absorption coefficient of pure a-Ge given in ref. [16] with our pseudo-brewster and absorption data; the agreement is indeed very reasonable. This figure also includes data for the hydrogenated samples which indicate a rather peculiar behaviour: with increasing partial pressures of H_2 in the sputtering gas the absorption edge first shifts towards higher photon energies up to ~10% H_2 partial pressure and then reverses this trend. While no interpretation of this anomaly is available, it is somewhat similar to the behaviour observed for sputtered a-SiH_x [21].

4.3. Shape of the first-order spectra of a-Ge and a-Si

We have already mentioned that the LO and possibly also the LA structure become weaker as the hydrogen concentration increases (see figs. 2 and 4) while TA and TO remain nearly the same. Calculations by Yndurain and Sen [22] show that the existence of sharp LA and LO structures depends on the presence of six-fold rings in the amorphous network similar to those of the crystal. The presence of five-

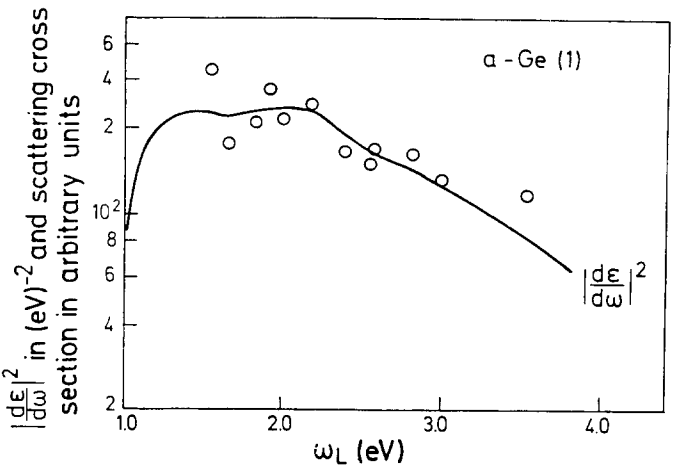

Fig. 10. Comparison of the resonant behaviour observed for the TO mode of pure a-Ge with the predictions of the dielectric theory $|d\epsilon/d\omega|^2$, with ϵ taken from ref. 16.

or seven-fold rings, as required by the Polk model of a-Si, and also the breaking up of the rings, as will be effected by hydrogen bonds, should tend to smear out the LA and LO structures. This phenomenon is formally analogous to the smearing out of the doublet structure observed in photoelectron spectra of crystalline Ge and Si 7 and 10 eV below the top of the valence bands [23,24].

Alben et al. have tried to interpret the shape of the first order spectra of pure

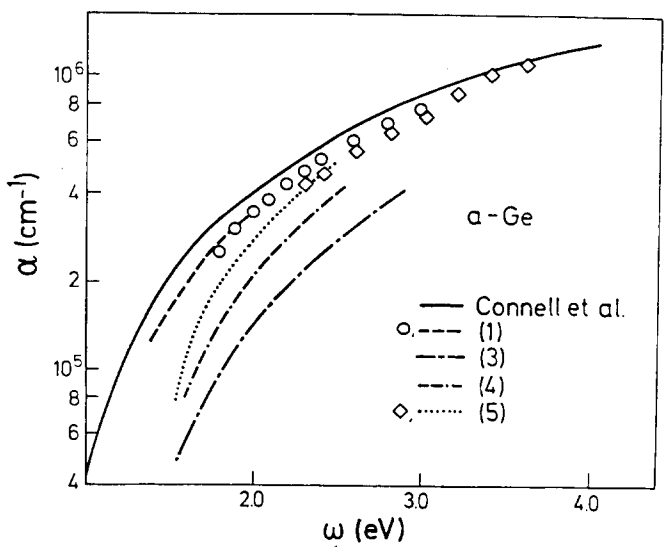

Fig. 11. Absorption coefficient of several pure and hydrogenated a-Ge samples obtained with the pseudo-brewster angle method (points) and by means of direct absorption measurements (dashed and dotted lines). The solid line represents the data of Connell et al. 16 for pure a-Ge.

a-Si on the basis of a simple bond polarizability model which assumes that a phonon induced distortion of a bond $\vec{u}_1$ produces the following changes in the polarizability tensor of that bond

$$\begin{aligned}
\overleftrightarrow{\alpha_1} &= \alpha_1 [\vec{r}_1\vec{r}_1 - \tfrac{1}{3}\overleftrightarrow{I}]\vec{u}_1 \cdot \vec{r}_1, \\
\overleftrightarrow{\alpha_2} &= \alpha_2 [\tfrac{1}{2}(\vec{r}_1\vec{u}_1 + \vec{u}_1\vec{r}_1) - \tfrac{1}{3}\overleftrightarrow{I}\,\vec{u}_1 \cdot \vec{r}_1], \\
\overleftrightarrow{\alpha_3} &= \alpha_3 \overleftrightarrow{I}\,\vec{u}_1 \cdot \vec{r}_1,
\end{aligned} \tag{3}$$

Where $\overleftrightarrow{I}$ is the unit dyadic $\vec{r}_1\vec{r}_1$ a diadic product and $\vec{r}_1$ the unit vector along the bond. The terms $\overleftrightarrow{\alpha_1}$ and $\overleftrightarrow{\alpha_3}$ correspond to bond stretching whereas $\overleftrightarrow{\alpha_2}$ has a bond stretching and a bond bending component. The terms $\overleftrightarrow{\alpha_1}$ and $\overleftrightarrow{\alpha_2}$ are responsible for the completely depolarized component of the spectrum ($\rho = \frac{3}{4}$) while $\overleftrightarrow{\alpha_3}$ is completely polarized. On the basis of an incorrect experimental value of $\rho(\rho \approx 0.8)$ Alben et al. [8] concluded that $\alpha_3 = 0$ and interpreted the experimental data with a mixture of $\overleftrightarrow{\alpha_1}$ and $\overleftrightarrow{\alpha_3}$ terms fitted basically to the ratio of the strengths of the observed TO and TA peaks. Because of our value of $\rho \approx 0.42$ at 1.55 eV (away from resonance) in Si (for Ge $\rho \approx 0.48$ at 1.8 eV) we have to revise this interpretation.

We first note that the bond stretching terms $\overleftrightarrow{\alpha_1}$ and $\overleftrightarrow{\alpha_3}$ will give scattering cross sections proportional to the average square fluctuation in bond length induced by the phonons. On the basis of a simple model Alben et al. [8] concluded that this square fluctuation was approximately proportional to the square of the phonon frequency times the square of the average amplitude of the phonon coordinate throughout the whole phonon spectrum. Hence $\overleftrightarrow{\alpha_1}$ and $\overleftrightarrow{\alpha_3}$ are expected to yield Raman spectra of the same shape and with a ratio of TO to TA strengths:

$$\frac{I_{\mathrm{TO}}}{I_{\mathrm{TA}}} = \frac{\omega_{\mathrm{TO}}\, n_{\mathrm{B}}(\mathrm{TO}) + 1}{\omega_{\mathrm{TA}}\, n_{\mathrm{B}}(\mathrm{TA}) + 1} = \begin{cases} 1.5 \text{ for Ge} \\ 2.3 \text{ for Si} \end{cases} \tag{4}$$

at room temperature. The experimental value of $I_{\mathrm{TO}}/I_{\mathrm{TA}}$ obtained from figs. 1 and 6 is affected by an uncertaintly in the definition of the background. For Ge, however, it agrees within this uncertainty with the result of eq. (4). For Si the ratio $I_{\mathrm{TO}}/I_{\mathrm{TA}}$ is smaller than given in eq. (4) ($\approx$1.0), a fact which led Alben et al. to introduce an $\overleftrightarrow{\alpha_2}$ contribution which, as we see, is not required for Ge.

Under the assumption, certainly valid for a-Ge but probably not so for a-Si, that $\alpha_2 \approx 0$ we can derive the ratio α_3/α_1 from the polarization ratio ρ: [25]

$$\rho = \alpha_1^2/(5\alpha_3^2 + \tfrac{4}{3}\alpha_1^2). \tag{5}$$

From eq. (5) we find $\alpha_3/\alpha_1 = 0.5$ from $\rho = 0.42$ (at 1.55 eV for a-Si). We note in figs. 3 and 6 that the scattering cross sections of pure a-Ge and a-Si equal those of the crystalline material away from the resonances. It is, therefore, reasonable to compare the ratio α_3/α_1 with that needed to interpret the first- and second-order

Raman spectra of the crystalline materials [26]. From ref. 26 we find

$$\alpha_3 \propto a_1/a_q, \qquad \alpha_1 \propto 3a_{25}/a_q + 6, \tag{6}$$

where a_1 and a_{25} are the parameters designated as α_1 and α_{25} in ref. [26]. Replacing into eq. (6) the values of these parameters given in ref. [26] for the crystalline materials we find $\alpha_3/\alpha_1 = 0.7$ in Si. The same calculation yields for a-Ge ($\rho = 0.48$ at 1.8 eV) $\alpha_3/\alpha_1 \approx 0.4$ as compared with the value of 0.8 obtained for crystalline material [26]. In view of the crudeness of the assumptions involved we feel this ratio is in reasonable agreement with that required by the depolarization ratio of the first-order spectrum of the amorphous materials.

Acknowledgements

We would like to thank Dr. Marc Brodsky for a number of discussions and for supplying some of the a-Si samples, and Mr. Barynin for technical assistance in the preparation of the films.

References

[1] P.A. Temple and C.E. Hathaway, Phys. Rev. B7 (1973) 3685.
[2] M.A. Renucci, J.B. Renucci, R. Zeyher and M. Cardona, Phys. Rev. B10 (1974) 4309.
[3] J.B. Renucci, R.N. Tyte and M. Cardona, Phys. Rev. B11 (1975) 3885.
[4] For a review see M. Brodsky, Light Scattering in Solids, ed. by M. Cardona (Springer Verlag, 1975) p. 205.
[5] J.S. Lannin, Solid St. Commun. 12 (1973) 947.
[6] D. Bermejo, M. Cardona, and M.H. Brodsky, Amorphous and Liquid Semiconductors (University of Edinburgh, 1977) p. 343.
[7] A. Pinczuk and E. Burstein, ref. [4], p. 63.
[8] R. Alben, D. Weaire, J.E. Smith, Jr. and M.H. Brodsky, Phys. Rev. B11 (1975) 2271.
[9] W.E. Spear and P.G. LeComber, Solid St. Commun. 17 (1975) 1193.
[10] M.H. Brodsky, M. Cardona and J.J. Cuomo, Phys. Rev. B16 (1977) 3556; M.H. Brodsky, M.A. Frisch, J.F. Ziegler and W.A. Lanford, Appl. Phys. Lett. 30 (1977) 561.
[11] G.A.N. Connell and J.R. Pawlik, Phys. Rev. B13 (1976) 787.
[12] R.F. Potter, Phys. Rev. 150 (1966) 562.
[13] Taylor-Hobson, Tallysurf 10.
[14] R. Loudon, J. Phys. 26 (1965) 677.
[15] D.T. Pierce and W.E. Spicer, Phys. Rev. B8 (1972) 3017.
[16] G.A.N. Connell, R.J. Temkin and W. Paul, Adv. Phys. 22 (1973) 643.
[17] G.J. Buchenauer, F.H. Pollak and M. Cardona, Phys. Rev. B3 (1971) 2504.
[18] L. Pauling, the Nature of the Chemical Bond (Cornell University Press, 1967) p. 226.
[19] M. Cardona, ref. [4], p. 10.
[20] K.H. Ho, M.L. Cohen and M. Schlüter, Phys. Rev. 15 (1977) 3888.
[21] D.A. Anderson, T.D. Mustakas and W. Paul, ref. [6], p. 334.
[22] F. Yndurain and P.N. Sen, Phys. Rev. B14 (1976) 531.
[23] J. Joannopulos and M.L. Cohen, Solid State Physics, eds. F. Seitz, D. Turnbull, and H. Ehrenreich, vol. (Academic Press, New York).
[24] L. Ley and M. Cardona, Topics in Applied Physics, vol. 27 (Springer Verlag, Heidelberg) in press.
[25] M.M. Sushchinskii, Raman Spectra of Molecules and Crystals (Israel Program for Scientific Translations, New York, Jerusalem, London 1972) p. 13.
[26] S. Go, H. Bilz, and M. Cardona, Phys. Rev. Lett. 34 (1975) 580.